To appear in *Computer-Aided Design*

The Intersection of Two Ruled Surfaces*

Hee-Seok Heo*, Myung-Soo Kim*, and Gershon Elber+

* Department of Computer Science, POSTECH, Pohang 790-784, South Korea

+ Department of Computer Science, Technion, IIT, Haifa 32000, Israel

Abstract

This paper presents an efficient and robust algorithm that computes the intersection curve of two ruled surfaces. The surface intersection problem is reformulated as a zero-set finding problem for a bivariate function, which is also equivalent to the construction of an implicit curve in the plane. Each connected component of the surface intersection curve corresponds to a connected component in the zero-set, and vice versa, except for some singular points, redundant solutions, and degenerate cases. We also present algorithms that detect all these singular points, redundant solutions, and degenerate cases.

Keywords: Surface intersection, ruled surface, line geometry, variable elimination, bivariate functions, zero-set finding, adaptive B-spline subdivision

1 Introduction

The surface/surface intersection problem has attracted considerable research attention in geometric and solid modeling. Many algorithms have been suggested for intersecting two free-form surfaces. However, there has been no known algorithm that can compute the intersection curve of two arbitrary rational surfaces accurately, robustly, and efficiently, while requiring no user intervention [7].

The situation is much better when we restrict the domain of input surfaces to that of simple surfaces such as planes, natural quadrics (spheres, cylinders, cones), and tori.

*The research was supported in part by the Korean Ministry of Science and Technology under Grants 97-NS-01-05-A-02-A of STEP 2000, and by KOSEF (Korea Science and Engineering Foundation) under Grant 96-0100-01-01-2. A preliminary version of this paper appeared in Reference [6].

These surfaces, the so-called CSG primitives, are important in conventional solid modeling systems since they can represent a large number of simple mechanical parts. There are some geometric algorithms that can intersect two natural quadrics efficiently and robustly [10, 15]. In particular, Miller and Goldman [10] reduce the problem of detecting all degenerate conic sections to that of checking a few simple algebraic expressions formulated with the geometric parameters of input surfaces. Kim et al. [8] present a torus/sphere intersection algorithm that is based on a Configuration space transformation. The basic approach can be extended to the intersection of a torus with a cylinder, a cone, or another torus. Kim and Kim [9] present an algorithm that can detect and construct all degenerate conic sections (circles) in the intersection of a torus and a natural quadric. This algorithm also follows the principle of Miller and Goldman [10] in that all degenerate conic sections (circles) can be detected exactly by evaluating a few simple algebraic expressions.

This paper considers the intersection of two ruled surfaces. The problem is more difficult than the case of natural quadrics as general ruled surfaces may have considerably more complex shapes than planes, cylinders, and cones (which represent the simplest ruled surfaces). On the other hand, ruled surfaces are simpler than general free-form surfaces. Hence, there may be a compromise – we raise a question: Would it be possible to develop an intersection algorithm (for ruled surfaces) that performs much better than those for general free-form surfaces? This paper spells out an affirmative answer to this question.

Among ruled surfaces, developable surfaces form an important subclass since they are useful in sheet metal design and processing [11]. Every developable surface can be obtained as the envelope surface of a moving plane (under a one-parameter motion). Thus the Gauss map of a developable surface generates a spherical curve on the unit sphere. The intersection of two developable surfaces can be essentially reduced to that of two spherical curves (or even to that of two planar curves after stereographic projection) [1]. After the developable surfaces are subdivided at the ruling lines corresponding to the intersection points of their Gauss maps, there is no internal loop in the intersection of two surface subpatches thus subdivided. (Two surfaces may intersect in an internal loop only if their Gauss maps overlap [13].)

The Gauss map of a non-developable ruled surface is a spherical region on the unit sphere (rather than being a spherical curve). When two non-developable ruled surfaces intersect (almost) tangentially, their Gauss maps overlap even after many steps of subdivision. Thus it is not easy to take advantage of the simple structure of ruled surfaces when we apply conventional subdivision techniques to the intersection of non-developable

ruled surfaces. One may consider a conventional algebraic method instead: Convert one surface $S_1(u_1, v_1)$ into an implicit form $F(x, y, z) = 0$, and substitute the parametric equation $S_2(u_2, v_2) = (x(u_2, v_2), y(u_2, v_2), z(u_2, v_2))$ of the other surface into the implicit form; the result produces an algebraic equation in two variables: $F(u_2, v_2) = F(x(u_2, v_2), y(u_2, v_2), z(u_2, v_2)) = 0$. (Note that the two parameters u_2 and v_2 come from the same surface $S_2(u_2, v_2)$.) Unfortunately, even for ruled surfaces, the implicitization is a non-trivial task to implement [14]. Therefore, we need to consider a different method.

Given two ruled surfaces $S_1(u, s) = C(u) + s\mathbf{a}(u)$ and $S_2(v, t) = D(v) + t\mathbf{b}(v)$, our approach is based on a simple observation that the linear parameters s and t can be eliminated simultaneously in a straightforward manner. The result is an implicit equation in two variables: $\lambda(u, v) = 0$. (Note that the parameters u and v come from two different ruled surfaces $S_1(u, s)$ and $S_2(v, t)$, respectively.) When two ruling lines intersect, they determine a unique plane. Our physical interpretation is based on the linear dependence of three vectors: $\mathbf{a}(u)$, $\mathbf{b}(v)$, and $C(u) - D(v)$, which are all parallel to the plane determined by the two intersecting ruling lines. This geometric observation enables us to exercise more intuitive analysis of various redundant solutions and degenerate cases. The resulting constraint equation $\lambda(u, v) = 0$ is also identical to the Plücker condition of line geometry for the intersection of two lines in the space [12]. Consequently, our algorithm can be extended to the intersection of rational ruled surfaces as well.

Our algorithm may be classified as an algebraic method in the sense that, after some algebraic manipulations for variable elimination, the surface intersection problem is reduced to a simpler problem of computing an implicit curve $\lambda(u, v) = 0$ in the uv-plane (i.e., the zero-set of a bivariate function). In conventional algebraic methods, it is very difficult to keep track of numerical errors that propagate in the sequence of algebraic manipulations since algebraic terms and operations have no clear geometric meaning. In our method, there is a birational correspondence between the two sets of parameters: (u, v) and (u, v, s, t). Thus we can reliably measure the propagation of error and extract the regions that should be treated more carefully (i.e., the regions vulnerable to numerical inaccuracy and/or topological inconsistency). Numerical/topological ill-conditions are formulated in terms of other bivariate functions: $\Delta(u, v)$, $\delta_1(u, v)$, and $\delta_2(u, v)$, which are based on geometric measures such as parallelity and line distance.

The rest of this paper is organized as follows. In Section 2, we reduce the problem of intersecting two ruled surfaces into that of computing the zero-set of a bivariate function: $\lambda(u, v) = 0$. Moreover, we classify all redundant solutions of the zero-set. Section 3

considers the degenerate cases: $\lambda(u,v) \equiv 0$, in which the zero-set degenerates into the whole plane. Section 4 demonstrates some experimental results. Finally, in Section 5, we conclude this paper.

2 Problem Reduction

Let $S_1(u,s)$ and $S_2(v,t)$ be two ruled surfaces defined by

$$S_1(u,s) = C(u) + s\mathbf{a}(u), \tag{1}$$

$$S_2(v,t) = D(v) + t\mathbf{b}(v), \tag{2}$$

for some *directrix* curves $C(u)$ and $D(v)$, and *indicatrix* curves $\mathbf{a}(u) \neq \mathbf{0}$ and $\mathbf{b}(v) \neq \mathbf{0}$. In this paper, we assume that $\mathbf{a}(u)$, $\mathbf{b}(v)$, $C(u)$, and $D(v)$ are all rational curves. Let $L_1^u(s)$ denote the ruling line of $S_1(u,s)$ as given in Equation (1) at a fixed parameter u. Similarly, let $L_2^v(t)$ denote the ruling line of $S_2(v,t)$ at a fixed v. When the two surfaces $S_1(u,s)$ and $S_2(v,t)$ intersect, we have

$$S_1(u,s) = S_2(v,t),$$

and equivalently,

$$C(u) - D(v) = -s\mathbf{a}(u) + t\mathbf{b}(v). \tag{3}$$

That is, the vector $C(u) - D(v)$ is given as a linear combination of $\mathbf{a}(u)$ and $\mathbf{b}(v)$. Consequently, the three vectors $\mathbf{a}(u)$, $\mathbf{b}(v)$, and $C(u) - D(v)$ are linearly dependent and the following determinant must vanish:

$$\lambda(u,v) = \det\left(\mathbf{a}(u), \mathbf{b}(v), C(u) - D(v)\right) = 0.$$

2.1 Redundant Solutions

The condition of $\lambda(u,v) = 0$ is a necessary, but not sufficient, condition for two ruling lines $L_1^u(s)$ and $L_2^v(t)$ to intersect. The solution set of $\lambda(u,v) = 0$ may contain some redundant points that do not correspond to real, affine intersection points of the two ruled surfaces. We classify all possible redundant solutions below.

Each solution of $\lambda(u,v) = 0$ implies the linear dependency of three vectors $\mathbf{a}(u)$, $\mathbf{b}(v)$, and $C(u) - D(v)$:

$$c_1\mathbf{a}(u) + c_2\mathbf{b}(v) + c_3\left(C(u) - D(v)\right) = 0, \tag{4}$$

for some real values of c_1, c_2, c_3, not all of which are identically zero. If $c_3 \neq 0$, this implies the condition of Equation (3). Under this condition, the two ruling lines intersect and there is no redundant solution of $\lambda(u, v) = 0$.

Next, we consider the case of $c_3 = 0$. Equation (4) is then equivalent to

$$\mathbf{a}(u) = -\frac{c_1}{c_2}\mathbf{b}(v),$$

for some $c_1 \neq 0$ and $c_2 \neq 0$. Then, two ruling directions $\mathbf{a}(u)$ and $\mathbf{b}(v)$ are parallel or opposite. Note that the pair (u, v) satisfies the condition $\lambda(u, v) = 0$ regardless of whether the corresponding ruling lines $L_1^u(s)$ and $L_2^v(t)$ intersect. Therefore, the solution (u, v) is redundant if the vectors $\mathbf{a}(u)$ and $\mathbf{b}(v)$ are parallel/opposite, but the corresponding ruling lines do not overlap. The condition of $\mathbf{a}(u)$ and $\mathbf{b}(v)$ being parallel/opposite can be represented as the zero-set of another bivariate function:

$$\Delta(u, v) = \|\mathbf{a}(u) \times \mathbf{b}(v)\|^2 = \|\mathbf{a}(u)\|^2\|\mathbf{b}(v)\|^2 - \langle \mathbf{a}(u), \mathbf{b}(v)\rangle^2 = 0.$$

Note that the zero-set of $\Delta(u, v) = 0$ is totally contained in the zero-set of $\lambda(u, v) = 0$.

Two parallel ruling lines $L_1^u(s)$ and $L_2^v(t)$ overlap each other if and only if they are parallel (i.e., $\Delta(u, v) = 0$) and the difference vector $C(u) - D(v)$ is parallel/opposite to $\mathbf{a}(u)$ and $\mathbf{b}(v)$:

$$\begin{aligned}
\delta_1(u, v) &= \|\mathbf{a}(u) \times (C(u) - D(v))\|^2 \\
&= \|\mathbf{a}(u)\|^2\|C(u) - D(v)\|^2 - \langle \mathbf{a}(u), C(u) - D(v)\rangle^2 = 0, \\
\delta_2(u, v) &= \|\mathbf{b}(v) \times (C(u) - D(v))\|^2 \\
&= \|\mathbf{b}(v)\|^2\|C(u) - D(v)\|^2 - \langle \mathbf{b}(v), C(u) - D(v)\rangle^2 = 0.
\end{aligned}$$

Note that $\delta(u, v) = \delta_1(u, v)/\|\mathbf{a}(u)\|^2$ is the squared distance between the point $D(v)$ and the ruling line $L_1^u(s)$. Similarly, $\delta(u, v) = \delta_2(u, v)/\|\mathbf{b}(v)\|^2$ is the squared distance between the point $C(u)$ and the ruling line $L_2^v(t)$. Thus, the two lines $L_1^u(s)$ and $L_2^v(t)$ overlap each other if and only if $\Delta(u, v) = \delta_1(u, v) = \delta_2(u, v) = 0$ (equivalently, $\Delta(u, v) + \delta_1(u, v) + \delta_2(u, v) = 0$ since $\Delta(u, v), \delta_1(u, v), \delta_2(u, v) \geq 0$). Figures 1, 3, and 5 show some illustrative examples of intersecting two circular cones; also shown are their corresponding bivariate functions: $\Delta(u, v)$, $\delta_1(u, v)$, $\delta_2(u, v)$, and $\Delta(u, v) + \delta_1(u, v) + \delta_2(u, v)$, under some reparameterizations of u and v.

In summary, a solution of $\lambda(u, v) = 0$ is redundant (i.e., the ruling lines $L_1^u(s)$ and $L_2^v(t)$ do not intersect) if and only if $\Delta(u, v) = 0$ and $\Delta(u, v) + \delta_1(u, v) + \delta_2(u, v) \neq 0$ (equivalently, $\delta_1(u, v) \neq 0$ and $\delta_2(u, v) \neq 0$).

2.2 Birational Correspondence

When two ruling lines $L_1^u(s)$ and $L_2^v(t)$ intersect in a real, affine point, the two parameters s and t can be represented as rational bivariate functions of u and v (assuming that $\mathbf{a}(u)$, $\mathbf{b}(v)$, $C(u)$, and $D(v)$ are all rational curves). By taking inner products of Equation (3) with the vectors $-\mathbf{a}(u)$ and $\mathbf{b}(v)$, we obtain the following linear system of equations for s and t:

$$\begin{bmatrix} \|\mathbf{a}(u)\|^2 & -\langle \mathbf{a}(u), \mathbf{b}(v) \rangle \\ -\langle \mathbf{a}(u), \mathbf{b}(v) \rangle & \|\mathbf{b}(v)\|^2 \end{bmatrix} \begin{bmatrix} s \\ t \end{bmatrix} = \begin{bmatrix} \langle \mathbf{a}(u), D(v) - C(u) \rangle \\ \langle \mathbf{b}(v), C(u) - D(v) \rangle \end{bmatrix}.$$

When we have the condition $\Delta(u, v) \neq 0$ (i.e., the two vectors $\mathbf{a}(u)$ and $\mathbf{b}(v)$ are neither parallel nor opposite), this matrix equation is non-singular and there are unique rational solutions of $s(u, v)$ and $t(u, v)$:

$$s(u,v) = \frac{\|\mathbf{b}(v)\|^2 \langle \mathbf{a}(u), D(v) - C(u) \rangle + \langle \mathbf{a}(u), \mathbf{b}(v) \rangle \langle \mathbf{b}(v), C(u) - D(v) \rangle}{\|\mathbf{a}(u)\|^2 \|\mathbf{b}(v)\|^2 - \langle \mathbf{a}(u), \mathbf{b}(v) \rangle^2}, \tag{5}$$

$$t(u,v) = \frac{\|\mathbf{a}(u)\|^2 \langle \mathbf{b}(v), C(u) - D(v) \rangle + \langle \mathbf{a}(u), \mathbf{b}(v) \rangle \langle \mathbf{a}(u), D(v) - C(u) \rangle}{\|\mathbf{a}(u)\|^2 \|\mathbf{b}(v)\|^2 - \langle \mathbf{a}(u), \mathbf{b}(v) \rangle^2}. \tag{6}$$

Note that the computation of $s(u, v)$ and $t(u, v)$ becomes quite unstable numerically when $\Delta(u, v) = \|\mathbf{a}(u) \times \mathbf{b}(v)\|^2 \approx 0$ (i.e., when the two ruling lines $L_1^u(s)$ and $L_2^v(t)$ are almost parallel). In this case, we measure the squared distance $\delta(u, v)$ between two almost parallel ruling lines and discard the lines if their squared distance is larger than a certain tolerance: $\delta(u, v) \geq \epsilon^2$.

The real difficulty arises when there are pairs of (almost) parallel ruling lines that (almost) overlap each other: i.e., $\Delta(u, v) + \delta_1(u, v) + \delta_2(u, v) \approx 0$. In this case, we may include either $L_1^u(s)$ or $L_2^v(t)$ in the intersection curve. When there are infinitely many solutions (thus forming a solution curve) of $\Delta(u, v) + \delta_1(u, v) + \delta_2(u, v) = 0$, the two ruled surfaces $S_1(u, s)$ and $S_2(v, t)$ overlap each other. A small perturbation in geometric data would change the intersection curve into a totally different one. The case of tangential intersection is extremely difficult to deal with in a topologically reliable manner (in particular, due to numerical error). A reliable solution for this case remains a challenging open problem for future research.

Let $\hat{C}$ be a segment of the intersection curve of $S_1(u, s)$ and $S_2(v, t)$, and C be its projection onto the uv-plane. (We assume that the two ruled surfaces do not overlap.) If $\hat{C}$ is a connected curve segment, C is a connected segment of the implicit curve: $\lambda(u, v) = 0$. But, the converse is not true in general. When a connected curve segment C of the

implicit curve $\lambda(u,v) = 0$ contains a point (u,v) of $\Delta(u,v) = 0$, there is no unique solution for $(s(u,v), t(u,v))$. Moreover, in some degenerate cases (to be discussed later), the intersection curve may be empty or just a single point, whereas the zero-set of $\lambda(u,v) \equiv 0$ is the whole plane. In these special cases, there is no correspondence between an intersection curve $\hat{C}$ and a segment C of the implicit curve $\lambda(u,v) = 0$. In general, with the exception of: (i) parallel ruling lines (i.e., $\Delta(u,v) = 0$), (ii) degenerate cases (i.e., $\lambda(u,v) \equiv 0$), and (iii) apexes and self-intersections (more details of which to be discussed below), we have birational correspondence between the intersection curve $\hat{C}$ and its projection C on the implicit curve $\lambda(u,v) = 0$.

Assume that the surface $S_1(u,s)$ has an apex P such that $S_1(u,s) = P$, for $u_0 \leq u \leq u_1$, and the apex P is located on the other surface: $P = S_2(v_0, t_0)$. Then the zero-set of $\lambda(u,v) = 0$ contains a line segment: $\{(u, v_0) |\ u_0 \leq u \leq u_1\}$. The whole line segment (in the uv-domain) corresponds to a single point P in the intersection of two ruled surfaces $S_1(u,s)$ and $S_2(v,t)$. Next, consider the case in which a self-intersection point Q of $S_1(u,s)$ is contained in the other surface $S_2(v,t)$; that is, Q is in the intersection curve: $Q = S_1(u_1, s_1) = S_1(u_2, s_2) = S_2(v_1, t_1)$. Two different solutions (u_1, v_1) and (u_2, v_1) (of $\lambda(u,v) = 0$) correspond to the same intersection point Q. Thus there is no birational correspondence between C and $\hat{C}$, in these cases, either.

All singular points of a ruled surface $S_1(u,s) = C(u) + s\mathbf{a}(u)$ must be located along its *striction* curve [2]:

$$\bar{C}(u) = C(u) - \frac{\langle C'(u), \bar{\mathbf{a}}'(u) \rangle}{\langle \bar{\mathbf{a}}'(u), \bar{\mathbf{a}}'(u) \rangle} \bar{\mathbf{a}}(u),$$

where $\bar{\mathbf{a}}(u) = \mathbf{a}(u)/\|\mathbf{a}(u)\|$ and $\bar{\mathbf{a}}'(u) = (\langle \mathbf{a}(u), \mathbf{a}(u) \rangle \mathbf{a}'(u) - \langle \mathbf{a}'(u), \mathbf{a}(u) \rangle \mathbf{a}(u))/\|\mathbf{a}(u)\|^3$. Note that $\bar{C}(u)$ is a rational curve when the given curves $C(u)$ and $\mathbf{a}(u)$ are rational. If the curve $\bar{C}(u)$ degenerates into a point, this point will be the apex of a conical surface $S_1(u,s)$. Assuming that the ruled surface $S_1(u,s)$ is noncylindrical, all singular points of $S_1(u,s)$ can be detected along the striction curve $\bar{C}(u)$ by testing the following condition [2]:

$$\left\langle \bar{C}'(u) \times \bar{\mathbf{a}}(u), \bar{\mathbf{a}}'(u) \right\rangle = 0,$$

or equivalently

$$\langle C'(u) \times \mathbf{a}(u), \mathbf{a}'(u) \rangle = 0.$$

Self-intersection points of $S_1(u,s)$ can be detected by intersecting $S_1(u,s)$ with $S_1(v,t)$ (i.e., the same surface as $S_1(u,s)$, but under different parameter naming). The diagonal line: $u - v = 0$ is contained in the zero-sets of all bivariate functions considered above. By

deleting the diagonal line from these zero-sets, we can characterize the self-intersection of a ruled surface $S_1(u, s)$.

2.3 Illustrative Examples

In this subsection, we consider three simple examples that illustrate typical types of redundant solutions. General ruled surfaces produce bivariate functions $\lambda(u, v)$, $\Delta(u, v)$, $\delta_1(u, v)$, $\delta_2(u, v)$ of high degree; thus, for the sake of simplicity, we employ circular cones and elliptic cylinders only. In each example, the unit circle has the following simple rational parameterization:

$$C(u) = \left(\frac{1-u^2}{1+u^2}, \frac{2u}{1+u^2}\right), \quad \text{for } -\infty < u < \infty. \tag{7}$$

Note that $(-1, 0)$ is missing from this parameterization. To remedy this, we may cover only half of the circle using this parameterization and cover the other half by reflecting the parameterization about the y-axis. For the convenience of presentation, we assume the parameterization of Equation (7), while special treatments are made for the missing point $(-1, 0)$ only when necessary.

In Equation (7), the parameter u is defined on an infinite domain. For the display of global function shape, we use another parameterization $\bar{u}$ (restricted to a bounded domain):

$$u = \frac{2\bar{u} - 1}{2\bar{u}(1-\bar{u})}, \quad \text{for } 0 < \bar{u} < 1.$$

Note that u is a strictly increasing rational function of $\bar{u}$. One may use $(\cos\theta, \sin\theta)$ to parameterize the unit circle on the domain $[0, 2\pi]$; however, the non-algebraic functions, sine and cosine, make some expressions too complex to be processed symbolically (even though they sometimes greatly simplify certain expressions).

Example 1: Let two ruled surfaces $S_1(u, s) = C(u) + s\mathbf{a}(u)$ and $S_2(v, t) = D(v) + t\mathbf{b}(v)$ be defined by four rational curves $\mathbf{a}(u)$, $\mathbf{b}(v)$, $C(u)$, and $D(v)$:

$$\mathbf{a}(u) = \left(\frac{1-u^2}{1+u^2}, \frac{2u}{1+u^2}, 1\right), \quad \mathbf{b}(v) = \left(\frac{1-v^2}{1+v^2}, \frac{2v}{1+v^2}, 1\right),$$
$$C(u) = \left(\frac{1-u^2}{1+u^2}, \frac{2u}{1+u^2}, 1\right), \quad D(v) = \left(\frac{2}{1+v^2}, \frac{2v}{1+v^2}, 1\right).$$

Note that $S_1(u, s)$ is a circular cone with its apex at $(0, 0, 0)$ and $S_2(v, t)$ is a simple translation of $S_1(u, s)$ by $(1, 0, 0)$ (see Figure 1(a)). From the above information, we get

the following bivariate functions:

$$\begin{aligned}
\lambda(u,v) &= \frac{2(u-v)(uv-1)}{(1+u^2)(1+v^2)}, \\
\Delta(u,v) &= \left\| \frac{2(u-v)\,(1-uv,\, u+v,\, -1-uv)}{(1+u^2)(1+v^2)} \right\|^2, \\
\delta_1(u,v) &= \left\| (0,-1,0) + \frac{2\,(-(1-uv)(u-v),\, -(u-v)(u+v),\, u(1+uv)+(u-v))}{(1+u^2)(1+v^2)} \right\|^2, \\
\delta_2(u,v) &= \left\| (0,-1,0) + \frac{2\,(-(1-uv)(u-v),\, -(u-v)(u+v),\, v(u-v)+(1+uv))}{(1+u^2)(1+v^2)} \right\|^2.
\end{aligned}$$

The real, affine solutions of $\lambda(u,v)=0$ generate a planar curve: $(u-v)(uv-1)=0$, whereas the solutions of $\Delta(u,v)=0$ generate a straight line: $u-v=0$. Thus the zero-set of $\Delta(u,v)=0$ is totally contained in that of $\lambda(u,v)=0$. It is easy to check that $\Delta(u,v)+\delta_1(u,v)+\delta_2(u,v)>0$, for all (u,v). Therefore, all solutions of $\Delta(u,v)=0$ are redundant solutions of $\lambda(u,v)=0$.

Figures 1(b)–1(f) show the bivariate functions: $\lambda(\bar{u},\bar{v})$, $\Delta(\bar{u},\bar{v})$, $\delta_1(\bar{u},\bar{v})$, $\delta_2(\bar{u},\bar{v})$, and $\Delta(\bar{u},\bar{v})+\delta_1(\bar{u},\bar{v})+\delta_2(\bar{u},\bar{v})=0$, under the reparameterizations: $u=\frac{2\bar{u}-1}{2\bar{u}(1-\bar{u})}$ and $v=\frac{2\bar{v}-1}{2\bar{v}(1-\bar{v})}$, for $0<\bar{u},\bar{v}<1$. Figure 1(f) shows that $\Delta(\bar{u},\bar{v})+\delta_1(\bar{u},\bar{v})+\delta_2(\bar{u},\bar{v})>0$, for all $0<\bar{u},\bar{v}<1$. Figures 2(b) and 2(c) show the zero-sets of $\lambda(u,v)=0$ and $\Delta(u,v)=0$. Non-redundant solutions of $\lambda(u,v)=0$ are shown in Figure 2(d).

The non-redundant solution set $C=\{(u,v)|\ \lambda(u,v)=0,\ \Delta(u,v)\neq 0\}$ is composed of four connected components in the uv-plane: $C_1=\{(u,v)|\ uv=1,\ u<-1\}$, $C_2=\{(u,v)|\ uv=1,\ -1<u<0\}$, $C_3=\{(u,v)|\ uv=1,\ 0<u<1\}$, and $C_4=\{(u,v)|\ uv=1,\ u>1\}$. At a first glance, one may think that there are only two connected components in the intersection curve of the two circular cones: one above the xy-plane and the other below the xy-plane (see Figure 1(a)). In our rational parameterizations of $S_1(u,s)$ and $S_2(v,t)$, one line of each cone is missing. (Note that the rational parameterization $\left(\frac{1-u^2}{1+u^2},\frac{2u}{1+u^2}\right)$ does not cover the point $(-1,0)$.) Thus the intersection curve consists of four connected components, each of which is in birational correspondence with C_i, for some $i=1,2,3,4$. (We may avoid this problem of a missing point by using a different parameterization of the unit circle; however, this will make our presentation lengthy. In the implementation of our algorithm, we approximate the unit circle with four cubic Bézier curve segments; see Figure 10.)

Note that two points $(1,1)$ and $(-1,-1)$ are limit points of C, but they are not in the solution set C. In a small neighborhood of these limit points (i.e., $\Delta(u,v)\approx 0$), the parameter values of $s(u,v)$ and $t(u,v)$ diverge to $\pm\infty$ (see Equations (5)–(6)). In

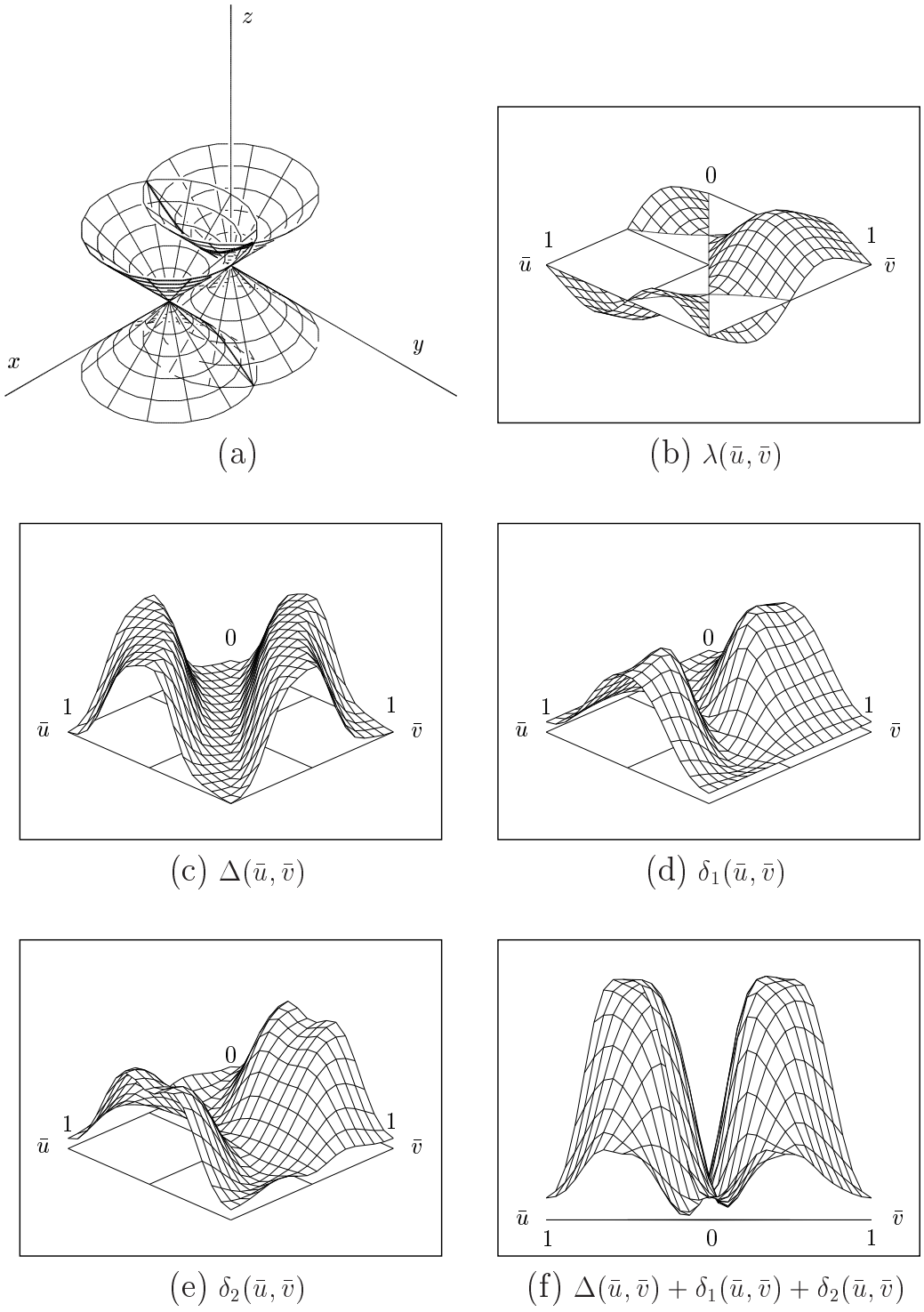

Figure 1: Bivariate Functions of Example 1.

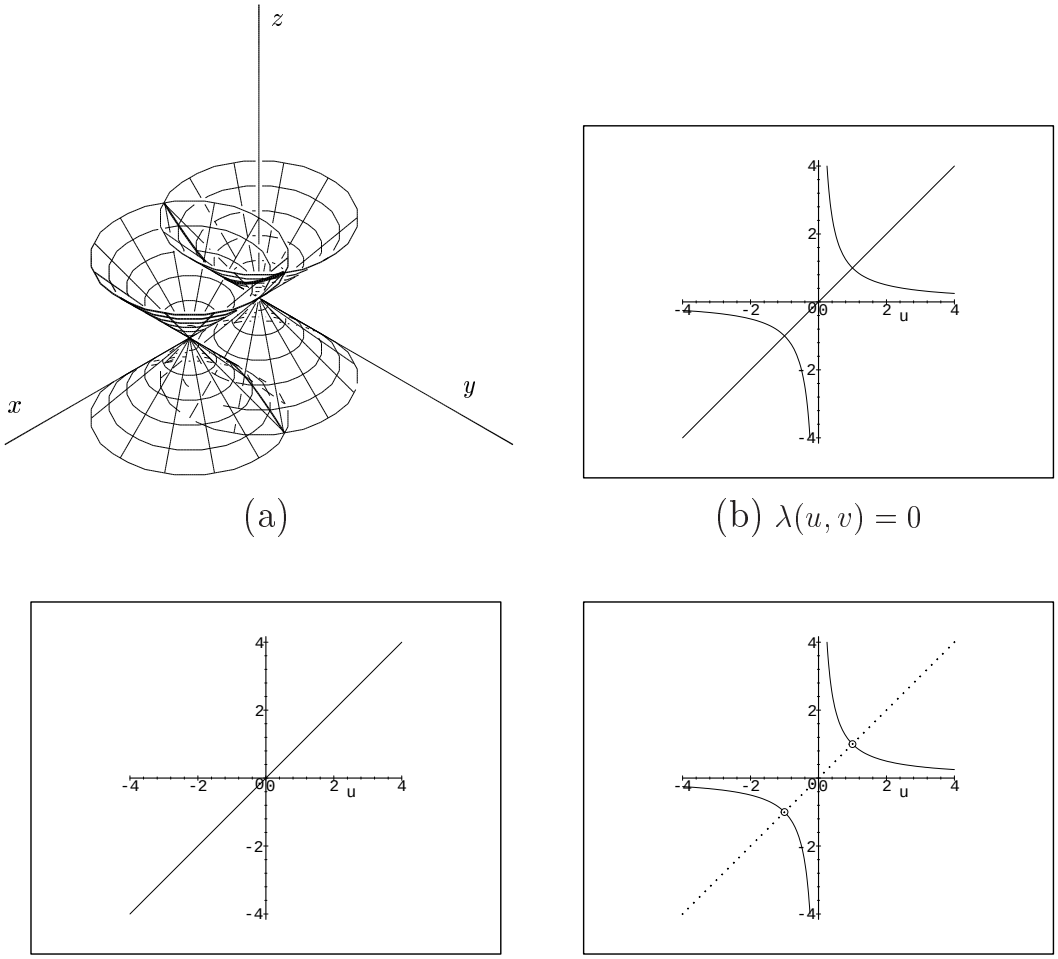

(a)

(b) $\lambda(u, v) = 0$

(c) $\Delta(u, v) = 0$

(d) Non-Redundant Solutions

Figure 2: Zero-Sets of Example 1.

practice, we use finite surface patches of circular cones. Thus the parameter values of s and t will be bounded. The solutions of (u, v) (near to $(\pm 1, \pm 1)$) can be ignored when their corresponding values of (s, t) are out of the bounded range.

Example 2: Let two ruled surfaces $S_1(u, s) = C(u) + s\mathbf{a}(u)$ and $S_2(v, t) = D(v) + t\mathbf{b}(v)$ be defined by:

$$\mathbf{a}(u) = \left(\frac{1-u^2}{1+u^2}, \frac{2u}{1+u^2}, 1\right), \quad \mathbf{b}(v) = \left(\frac{1-v^2}{1+v^2}, \frac{2v}{1+v^2}, 1\right),$$
$$C(u) = \left(\frac{1-u^2}{1+u^2}, \frac{2u}{1+u^2}, 1\right), \quad D(v) = \left(\frac{1-v^2}{1+v^2}, \frac{(1+v)^2}{1+v^2}, 0\right).$$

Note that $S_2(v, t)$ is a simple translation of $S_1(u, s)$ by $(0, 1, -1)$ (see Figure 3(a)). From the above information, we get the following bivariate functions:

$$\begin{aligned}
\lambda(u,v) &= \frac{2(1+u)(1+v)(v-u)}{(1+u^2)(1+v^2)}, \\
\Delta(u,v) &= \left\| \frac{2(u-v)\,(1-uv, u+v, -1-uv)}{(1+u^2)(1+v^2)} \right\|^2, \\
\delta_1(u,v) &= \left\| \left(\frac{(1+v)^2}{1+v^2}, \frac{(v-1)(1+v)}{1+v^2}, \frac{(1+v)(vu^2-2uv-v+u^2-1+2u)}{(1+u^2)(1+v^2)} \right) \right\|^2, \\
\delta_2(u,v) &= \left\| (1,1,0) + \left(\frac{4v}{1+v^2} - \frac{2u}{1+u^2}, \frac{2}{1+u^2} - \frac{4}{1+v^2}, \right. \right. \\
&\qquad \left. \left. \frac{(u-1)(2uv+uv^2-u-v^2+1+2v)}{(1+u^2)(1+v^2)} \right) \right\|^2.
\end{aligned}$$

The solutions of $\lambda(u, v) = 0$ generate a planar curve: $(u-v)(u+1)(v+1) = 0$, whereas the solutions of $\Delta(u, v) = 0$ generate a straight line: $u - v = 0$; see Figure 4(b). Moreover, it is easy to check that $(-1, -1)$ is the only common solution of $\Delta(u, v) = \delta_1(u, v) = \delta_2(u, v) = 0$; thus the solution $(-1, -1)$ is not a redundant solution of $\lambda(u, v) = 0$.

The non-redundant solution set $C = \{(u, v)|\ (u + 1)(v + 1) = 0\}$ is composed of two lines (vertically intersecting) in the uv-plane (see Figure 4(d)). Let $C_1 = \{(u, v)|\ u < -1,\ v = -1\}$, $C_2 = \{(u, v)|\ u > -1,\ v = -1\}$. $C_3 = \{(u, v)|\ u = -1,\ v < -1\}$, and $C_4 = \{(u, v)|\ u = -1,\ v > -1\}$. All solutions (u, v) in the set $C_1 \cup C_2$ correspond to the same intersection point $(0, 0, 0)$; that is, all ruling lines $L_1^u(s)$ of $S_1(u, s)$ intersect with the line $L_2^{-1}(t)$ at the common intersection point $(0, 0, 0)$, which is also the apex of $S_1(u, s)$. Similarly, all solutions (u, v) in the set $C_3 \cup C_4$ correspond to the same intersection point $(0, 1, -1)$, which is the apex of $S_2(v, t)$. The point $(-1, -1)$ corresponds to the pair of ruling lines $L_1^{-1}(s)$ and $L_2^{-1}(t)$ that overlap in the same line: $\{(0, t, -t)|\ -\infty < t < \infty\}$.

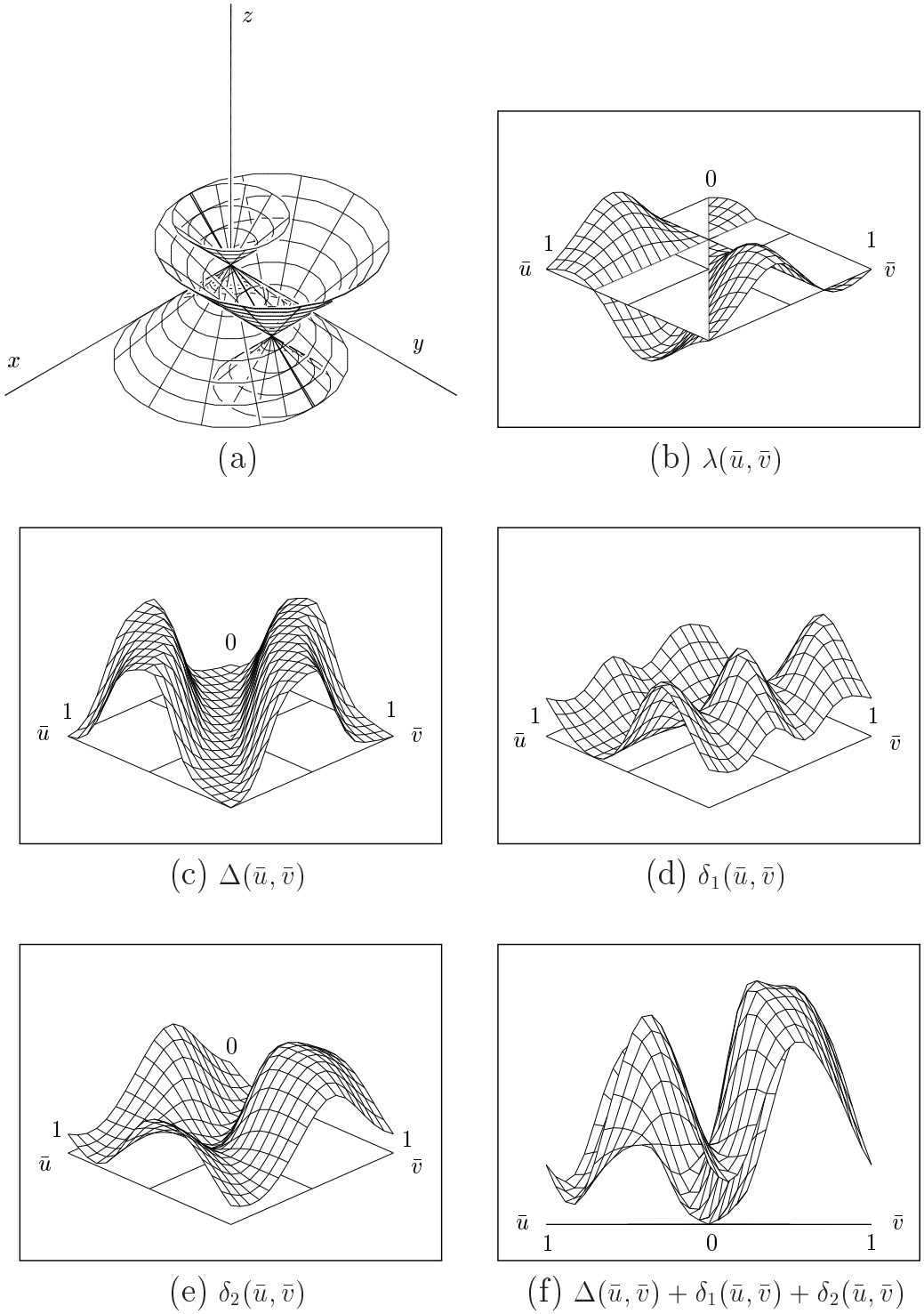

Figure 3: Bivariate Functions of Example 2.

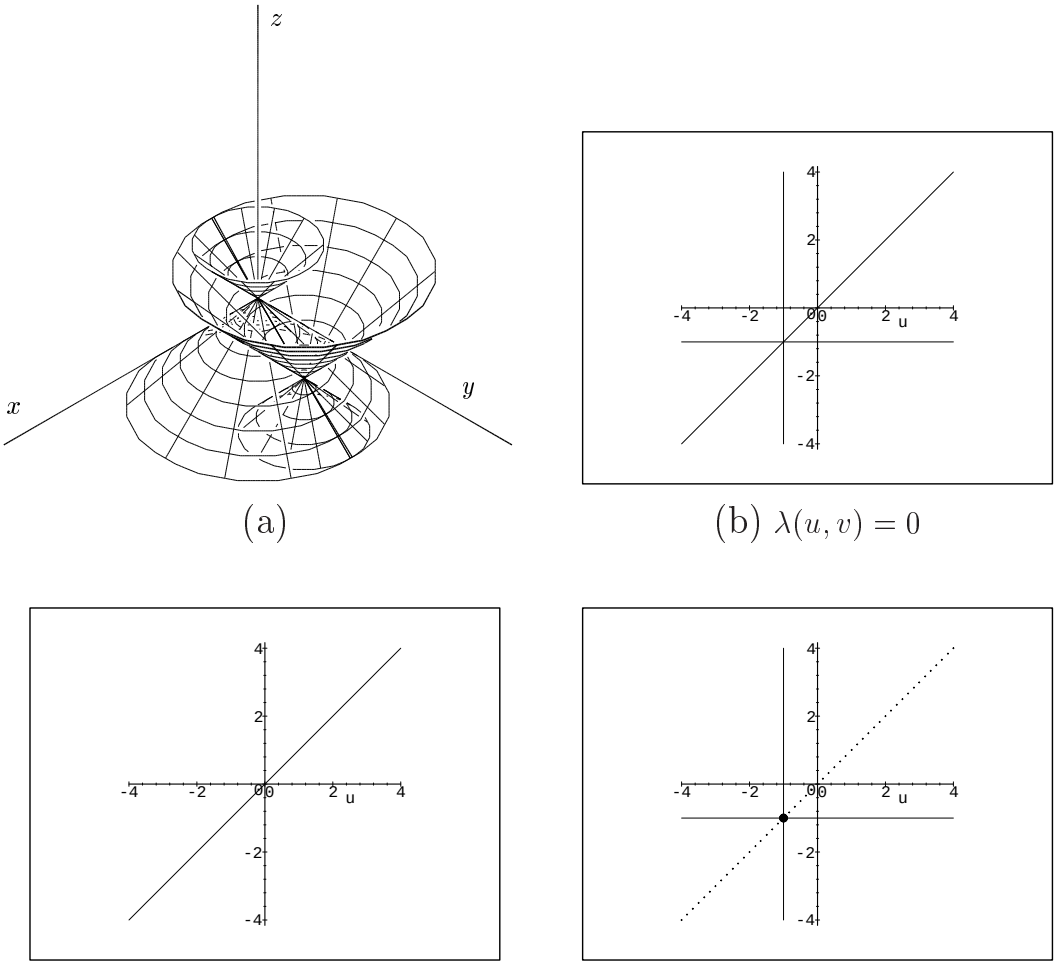

(a)

(b) $\lambda(u, v) = 0$

(c) $\Delta(u, v) = 0$

(d) Non-Redundant Solutions

Figure 4: Zero-Sets of Example 2.

In summary, the two circular cones $S_1(u,s)$ and $S_2(v,t)$ intersect tangentially along a line. There are no other intersection points.

In this example, there is no birational correspondence between each solution set C_i ($i = 1,2,3,4$) and a connected component of the intersection curve; instead they correspond to the apexes $(0,0,0)$ and $(0,1,-1)$ of the input surfaces $S_1(u,s)$ and $S_2(v,t)$, respectively.

Example 3: Let two ruled surfaces $S_1(u,s) = C(u) + s\mathbf{a}(u)$ and $S_2(v,t) = D(v) + t\mathbf{b}(v)$ be defined by:

$$\begin{aligned}
\mathbf{a}(u) &= \left(\frac{1-u^2}{1+u^2}, \frac{2u}{1+u^2}, 1\right), \quad \mathbf{b}(v) = (0,1,1), \\
C(u) &= \left(\frac{1-u^2}{1+u^2}, \frac{2u}{1+u^2}, 1\right), \quad D(v) = \left(\frac{1-v^2}{1+v^2}, \frac{2v}{1+v^2}, 1\right).
\end{aligned}$$

Note that $S_1(u,s)$ and $S_2(v,t)$ share the same directrix circle (see Figure 5(a)). Moreover, the two surfaces are tangential along a line: $\{(0,t,t) | -\infty < t < \infty\}$. Since the circular cone $S_1(u,s)$ and the elliptic cylinder $S_2(v,t)$ are both quadric surfaces, their intersection curve has degree four at most. One circle and one tangent line (considered as two lines overlapping in the same line) form a curve of degree four. Consequently, it is clear that there are no other intersection points. From the above information, we get the following bivariate functions:

$$\begin{aligned}
\lambda(u,v) &= \frac{2(1-u)(1-v)(v-u)}{(1+u^2)(1+v^2)}, \\
\Delta(u,v) &= \left\| \frac{(1-u)\,(u-1, -(1+u), 1+u)}{1+u^2} \right\|^2, \\
\delta_1(u,v) &= \left\| (1-v)\left(\frac{v-1}{1+v^2}, \frac{-(1+v)}{1+v^2}, \frac{2uv+u^2v-v+u^2+1+2u}{(1+u^2)(1+v^2)}\right) \right\|^2, \\
\delta_2(u,v) &= \left\| \frac{2(u-v)\,(uv-1, -(u+v), u+v)}{(1+u^2)(1+v^2)} \right\|^2.
\end{aligned}$$

The solutions of $\lambda(u,v) = 0$ generate a planar curve: $(u-v)(u-1)(v-1) = 0$, whereas the solutions of $\Delta(u,v) = 0$ generate a straight line: $u-1 = 0$; see Figure 6. Moreover, it is easy to check that $(1,1)$ is the only common solution of $\Delta(u,v) = \delta_1(u,v) = \delta_2(u,v) = 0$. The non-redundant solution set $C = \{(u,v) |\ (u-v)(v-1) = 0\}$ is composed of two lines (intersecting at 45° angle) in the uv-plane. Let $C_1 = \{(u,v) |\ u = v,\ v < 1\}$, $C_2 = \{(u,v) |\ u = v,\ v > 1\}$, $C_3 = \{(u,v) |\ u < 1,\ v = 1\}$, and $C_4 = \{(u,v) |\ u > 1,\ v = 1\}$.

Each solution (u,v) in the set $C_1 \cup C_2$ corresponds to an intersection point on the unit circle $C(u)$, or equivalently on the same circle $D(v)$. Note that C_1 and C_2 are in birational

correspondences with circular arcs $\{(\cos\theta, \sin\theta, 1) | -\pi < \theta < \frac{\pi}{2}\}$ and $\{(\cos\theta, \sin\theta, 1) | \frac{\pi}{2} < \theta < \pi\}$, respectively. Nevertheless, there is no birational correspondence between C_i $(i = 3, 4)$ and a connected component of the intersection curve; they correspond to the apex $(0, 0, 0)$ of $S_1(u, s)$. The point $(1, 1)$ corresponds to the pair of ruling lines $L_1^1(s)$ and $L_2^1(t)$ that overlap in the same line: $\{(0, t, t) | \ -\infty < t < \infty\}$. In summary, the circular cone $S_1(u, s)$ and the elliptic cylinder $S_2(v, t)$ intersect in a circle and a tangent line. There are no other intersection points.

3 Degenerate Cases

When $\mathbf{a}(u), \mathbf{b}(v), C(u)$, and $D(v)$ are given as polynomial/rational curves, the solution set of $\lambda(u, v) = 0$ is a planar algebraic curve, in general. However, in some degenerate cases, the solution set may degenerate into the whole plane, i.e., $\lambda(u, v) \equiv 0$. For example, consider two parallel cylindrical surfaces for which $\mathbf{a}(u)$ and $\mathbf{b}(v)$ are constant and parallel (see Figure 7(a)). Then we have $\Delta(u, v) \equiv 0$, which implies $\lambda(u, v) \equiv 0$ as well. Moreover, consider two conical surfaces that share a single apex located at point P (see Figure 7(b)). Each ruling line $L_1^u(s)$ of $S_1(u, s)$ intersects with all other ruling lines $L_2^v(t)$ of $S_2(v, t)$ at the common apex P. Thus we have $\lambda(u, v) \equiv 0$. These two cases essentially cover all possible degenerate cases of $\lambda(u, v) \equiv 0$. The only exceptions are the cases in which two ruled surfaces overlap. Below we show that the two overlapping ruled surfaces must be planes or rational bilinear surfaces (quadrics). Consequently, the detection of all degenerate cases can be essentially reduced to the problem of classifying the special types of input surfaces: whether the surface is a plane, cylinder, cone, quadric, or something else. (See Elber and Kim [5] for some related algorithms that detect special types of free-form surfaces.)

When $\mathbf{a}(u)$ and $\mathbf{b}(v)$ are parallel/opposite for all pairs of (u, v) (i.e., $\Delta(u, v) \equiv 0$), the surfaces $S_1(u, s)$ and $S_2(v, t)$ are cylindrical surfaces which are parallel to each other. Otherwise, $\mathbf{a}(u)$ and $\mathbf{b}(v)$ are parallel/opposite only for the pairs of (u, v) satisfying the condition of $\Delta(u, v) = 0$. In general, $\Delta(u, v) = 0$ is an algebraic curve in the uv-plane, which cannot be a space-filling curve. Thus there is a region $[u_a, u_b] \times [v_a, v_b]$ in which $\Delta(u, v) \neq 0$, for all $(u, v) \in [u_a, u_b] \times [v_a, v_b]$. Since we assume $\lambda(u, v) \equiv 0$, $C(u) - D(v)$ must be given as a linear combination of $\mathbf{a}(u)$ and $\mathbf{b}(v)$, for all $u_a \leq u \leq u_b$ and $v_a \leq v \leq v_b$. Thus, we have

$$C(u) - D(v) = s(u, v)\mathbf{a}(u) + t(u, v)\mathbf{b}(v),$$

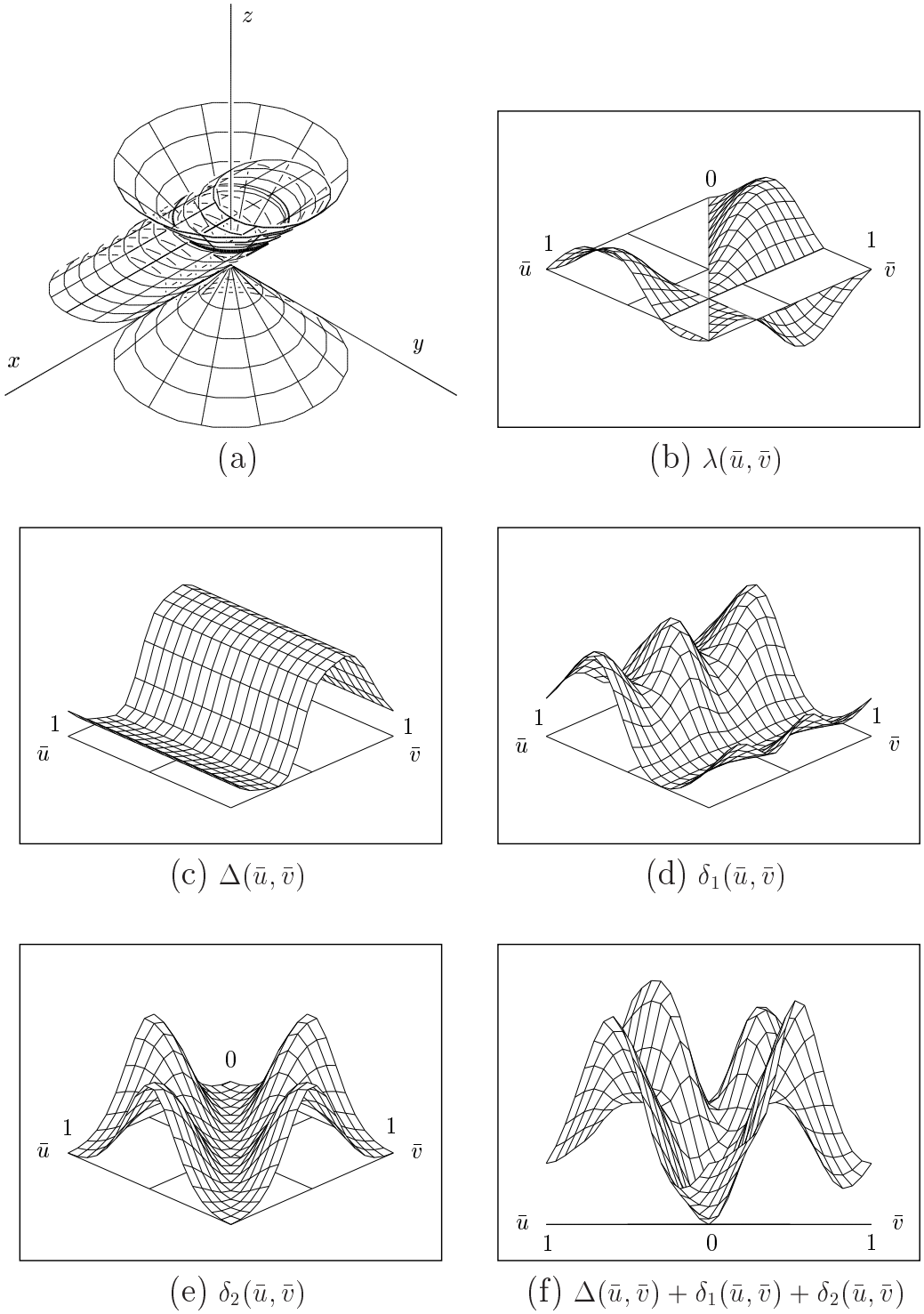

Figure 5: Bivariate Functions of Example 3.

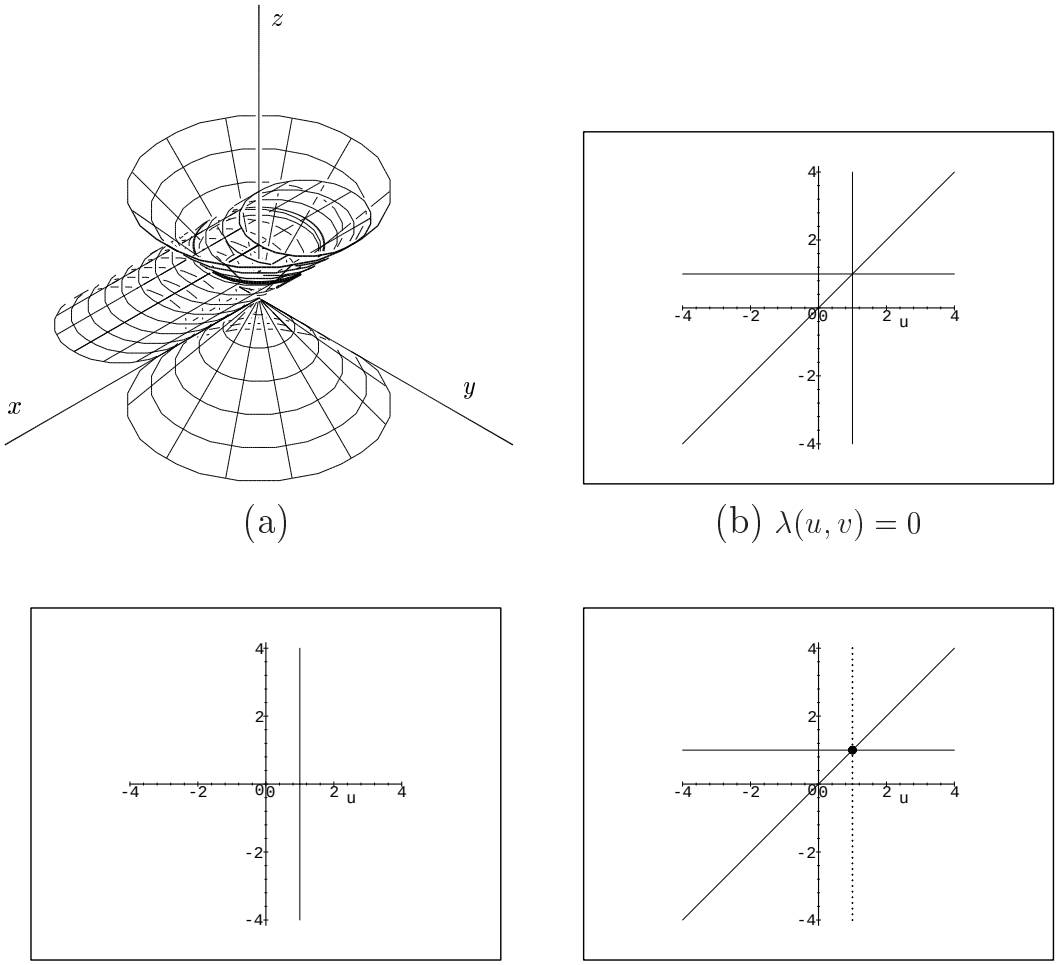

(a) (b) $\lambda(u, v) = 0$

(c) $\Delta(u, v) = 0$ (d) Non-Redundant Solutions

Figure 6: Zero-Sets of Example 3.

and equivalently,

$$C(u) + s(u,v)\mathbf{a}(u) = D(v) + t(u,v)\mathbf{b}(v),$$

for some real functions $s(u,v)$ and $t(u,v)$. This means that each ruling line $L_1^u(s)$ of $S_1(u,s)$ intersects with all other ruling lines $L_2^v(t)$ of $S_2(v,t)$, and vice versa. There are three different cases to consider (we assume $u_a \le u_0 < u_1 \le u_b$ and $v_a \le v_0 < v_1 \le v_b$):

- Case I: There exists a pair of lines $L_1^{u_0}(s)$ and $L_1^{u_1}(s)$ that intersect at a point P.

  Each ruling line $L_2^v(t)$ of $S_2(v,t)$ intersects with both $L_1^{u_0}(s)$ and $L_1^{u_1}(s)$. There are two subcases to consider:

  - If there are infinitely many $L_2^v(t)$ passing through the point P, the surface $S_2(v,t)$ must be a conical surface with its apex at P.
  - Otherwise, infinitely many lines $L_2^v(t)$ must be contained in the plane determined by $L_1^{u_0}(s)$ and $L_1^{u_1}(s)$. Then the whole surface $S_2(v,t)$ degenerates into a plane.

  The surface type of $S_1(u,s)$ is also determined in a similar way.

  - If $S_2(v,t)$ is a non-planar conical surface (with its apex at P), all ruling lines $L_1^u(s)$ of $S_1(u,s)$ pass through the apex P. Consequently, $S_1(u,s)$ also becomes a conical surface. (See Figure 7(b).)
  - Otherwise, $S_2(v,t)$ is a plane. All ruling lines $L_1^u(s)$ of $S_1(u,s)$ are contained in the plane of $S_2(v,t)$. Hence, $S_1(u,s)$ and $S_2(v,t)$ degenerate into the same plane. (See Figure 7(c).)

- Case II: There exists a pair of parallel lines $L_1^{u_0}(s)$ and $L_1^{u_1}(s)$.

  There is a unique plane determined by these two parallel lines. All ruling lines $L_2^v(t)$ of $S_2(v,t)$ are contained in the plane. Thus the whole surface $S_2(v,t)$ degenerates into the plane. Similarly, the other surface $S_1(u,s)$ is also contained in the same plane.

- Case III: Any two different lines $L_1^{u_0}(s)$ and $L_1^{u_1}(s)$ are skew.

  We may assume that any two different lines $L_2^{v_0}(t)$ and $L_2^{v_1}(t)$ are also skew. (Otherwise, we will end up with Case I or Case II considered above.) Let P_{uv} be the intersection point of two lines $L_1^u(s)$ and $L_2^v(t)$. Let $S(u,v) = P_{uv}$, for all $(u,v) \in [u_a, u_b] \times [v_a, v_b]$. Then $S_1(u,s)$ and $S_2(v,t)$ are coincident with the surface

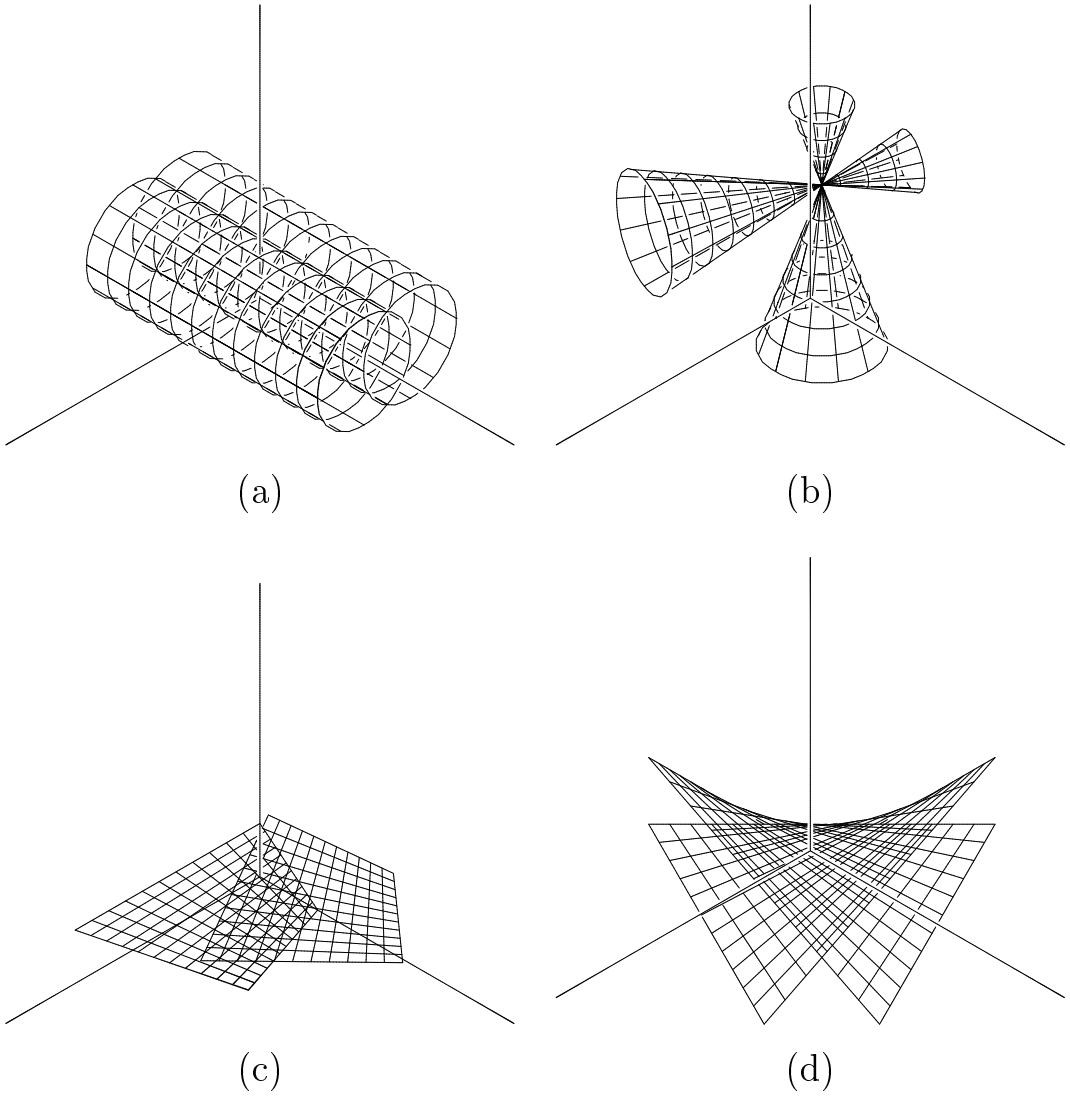

Figure 7: Degenerate Intersections.

$S(u, v)$; thus $S_1(u, s)$ and $S_2(v, t)$ are the same surface. In fact, $S(u, v)$ generates a rational bilinear surface under certain reparameterizations of u and v. Moreover, this surface must be a quadric surface. (See Appendices A and B for detailed proofs of these arguments.)

4 Experimental Results

The computation of bivariate functions $\lambda(u, v)$, $\Delta(u, v)$, $\delta_1(u, v)$, and $\delta_2(u, v)$ is quite simple and efficient. Using symbolic tools to compute the summation, difference, and product of (piecewise) polynomial/rational forms [3], we can derive (piecewise) polynomial func-

tions representing the numerators of $\lambda(u,v)$, $\Delta(u,v)$, $\delta_1(u,v)$, and $\delta_2(u,v)$. Figure 8(a) shows a simple example of intersecting two ruled surfaces that meet transversally. The corresponding bivariate function $\lambda(u,v)$ is shown in Figure 8(b). (In this example, the zero-set of $\Delta(u,v)=0$ is empty; thus the zero-set of $\lambda(u,v)=0$ contains non-redundant solutions only.)

An intersection curve is computed in three major steps:

1. formulate bivariate polynomial functions $\lambda(u,v)$, $\Delta(u,v)$, $\delta_1(u,v)$, and $\delta_2(u,v)$;
2. compute the zero-set of $\lambda(u,v)=0$, while excluding the solutions of $\Delta(u,v)=0$;
3. detect the pairs of overlapping ruling lines that correspond to the common solutions of $\Delta(u,v)=\delta_1(u,v)=\delta_2(u,v)=0$.

According to our experimental results, all three steps were found to be reasonably efficient. The symbolic computation of $\lambda(u,v)$, $\Delta(u,v)$, $\delta_1(u,v)$, and $\delta_2(u,v)$ took only a fraction of a second in all the examples demonstrated in this paper. The zero-set finding of $\lambda(u,v)=0$ (under the constraint $\Delta(u,v)\neq 0$) took a couple of seconds. In practice, we rarely have a solution of $\Delta(u,v)+\delta_1(u,v)+\delta_2(u,v)=0$. Except the case of two identical ruled surfaces overlapping each other, there would be only a few discrete solutions, if any, of this equation; the root finding procedure then converges very quickly to the discrete solutions.

The zero-set finding is essentially a computational procedure that requires finding all the points along the intersection curve between the graph surface $\mathcal{G}(u,v)=(u,v,\lambda(u,v))$ and the uv-plane. Thus the problem of intersecting two ruled surfaces has been reduced to a simpler yet another surface surface intersection (SSI) problem. Among numerous methods available for the SSI problem, subdivision-based methods produce the most reliable solutions, in general. They are usually slower than other sophisticated methods based on curve tracing. Quite often, other methods also take advantage of a preprocessing step that is based on subdivision. In this paper, due to robustness consideration, we adopt a subdivision-based scheme for finding the zero-set of $\lambda(u,v)=0$. (A similar technique is applied to the computation of the zero-sets of other bivariate functions.) As we have observed above, using this method, only a few seconds were required to construct each of the examples demonstrated in this paper. Therefore, the gain in robustness justifies our approach.

This robust adaptive subdivision approach depends on an ability to represent the bivariate functions $\lambda(u,v)$, $\Delta(u,v)$, $\delta_1(u,v)$, and $\delta_2(u,v)$ symbolically. By searching for the

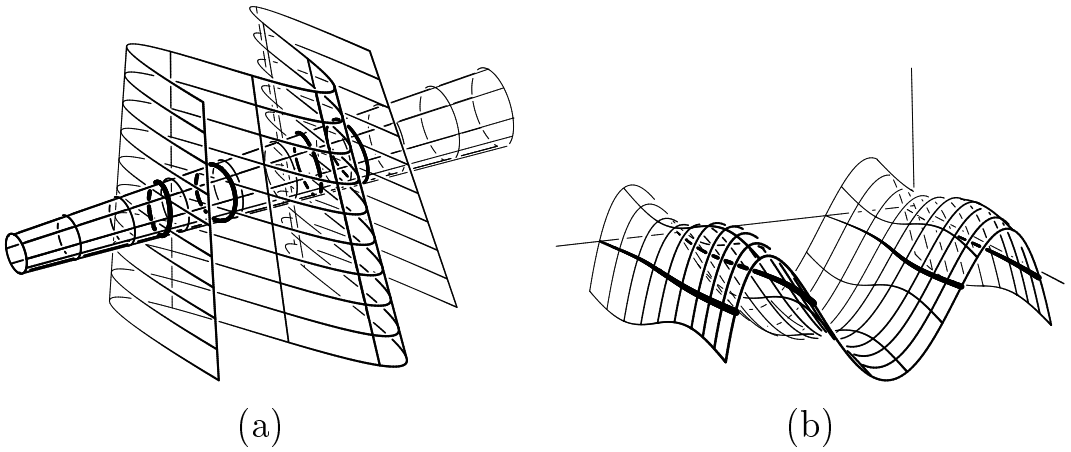

(a) (b)

Figure 8: Transversal intersection of two ruled surfaces in (a). In (b), the $\lambda(u, v)$ function is shown.

extreme control points of each surface subregion during the subdivision, and exploiting the convex hull property of the Bézier and B-spline representations, we can efficiently extract the surface subregions that intersect with the uv-plane. When the remaining surface patches become sufficiently flat, we triangulate these surface patches. The intersection of the triangulated surface with the uv-plane provides a polygonal approximation of the zero-set $\lambda(u, v) = 0$. We applied a numerical improvement procedure (based on local Newton-Raphson steps) to a piecewise linear approximation of the zero-set. Final results have very high precision, with typical tolerances of six orders of magnitude.

Figures 9(a)–9(d) show a sequence of examples that intersect two almost coaxial cylinders with angles of 10°, 1°, 0.1°, 0.01° between the two cylinders, in that order. Figures 9(e) and 9(f) are the λ-functions of the examples shown in Figures 9(a) and 9(d), respectively. It is very difficult to distinguish two intersecting cylinders that appear almost overlapping in Figures 9(c)–9(d). Moreover, the λ-function of Figure 9(f) is almost flat. Nevertheless, the computation results are numerically stable and they produce reasonable solutions, which demonstrates the robustness of our intersection algorithm for two ruled surfaces. The indicatrix curves $\mathbf{a}(u)$ and $\mathbf{b}(v)$ are constant for cylinders; thus the bivariate function $\Delta(u, v)$ also has a constant value for each of the examples shown in Figures 9(a)–9(d). In fact, we have $\Delta(u, v) = \sin^2\theta \approx 0.3 * 10^{-1}$, $0.3 * 10^{-3}$, $0.3 * 10^{-5}$, and $0.3 * 10^{-7}$, for the four examples. The values of $\delta_1(u, v)$ and $\delta_2(u, v)$ are also in similar ranges for the pairs (u, v) on the diagonal: $u - v = 0$. Thus we may regard the two cylinders of Figure 9(c) and 9(d) as almost overlapping.

Figures 11–13 show the experimental results of our algorithm applied to Examples

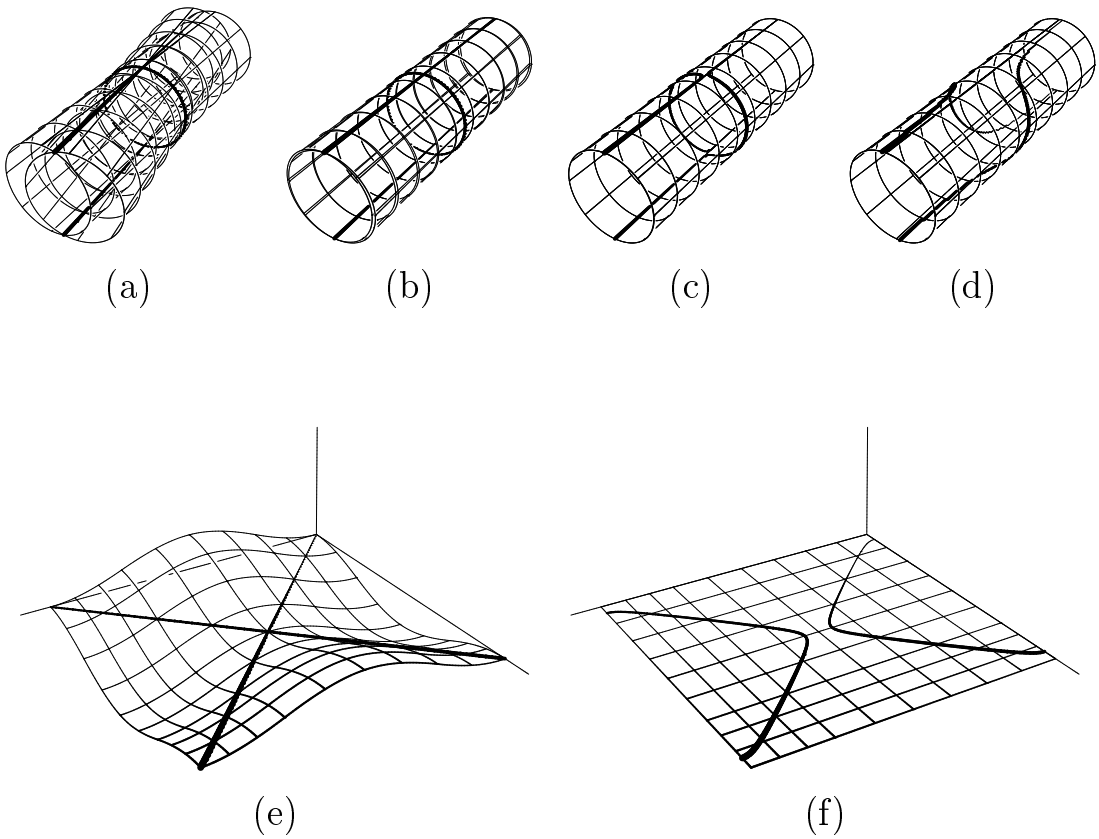

Figure 9: Intersection of two cylinders. In (a)-(d), two almost coaxial cylinders are intersected, with the angle between the two cylinders being 10°, 1°, 0.1°, 0.01°. In (e) and (f), the $\lambda(u, v)$ functions for cases (a) and (d) are shown.

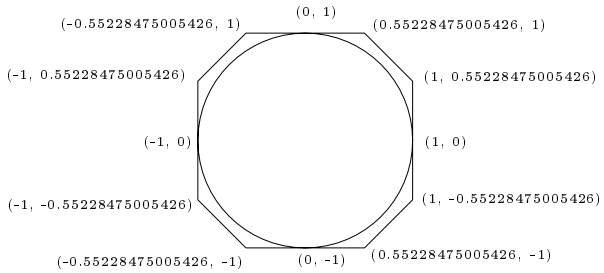

Figure 10: Circle Approximation with Four Cubic Bézier Curve Segements.

1–3 (see also Figures 1–6); the intersection curve of each example has been projected from the *uvst*-space to different domains so as to clarify its topological structure. The unit circle is approximated by four cubic Bézier curve segments as shown in Figure 10. (Each circular cone is thus approximated by four Bézier surface patches of degree $(3, 1)$.) Due to numerical error, it is very difficult to detect the exact lines and circles appearing in the intersection curves of Figures 12 and 13. Nevertheless, the computational results are very close to the exact intersection curves, which demonstrates the robustness of our intersection algorithm.

Figure 11(b) can be obtained by projecting the solution curves of Figure 11(e) or Figure 11(f) into the uv-plane. The curve segments have been trimmed off due to the limited ranges of s and t. Note that the (u, v) pairs near to the lines: $u = 0$, $v = 0$, and $u = v$, correspond to the positive/negative infinity of s and t values. In Figure 12, the intersection curve consists of three connected components; each segment is bounded by $(0, 0, 0)$ and/or $(0, 1, -1)$, the apexes of two circular cones. Note that two adjacent line segments are topologically connected at a common apex. The result of Figure 13 looks more interesting. Segment 1 consists of a half-line $\{(0, t, t) |\ t > 1\}$ and a three-quarter circle $\{(\cos\theta, \sin\theta, 1) |\ \pi/2 \leq \theta \leq 2\pi\}$, whereas segment 2 consists of the rest quarter circle $\{(\cos\theta, \sin\theta, 1) |\ 0 \leq \theta \leq \pi/2\}$, and a line segment $\{(0, t, t) |\ 0 \leq t \leq 1\}$. In fact, segments 1 and 2 are topologically connected at $(0, 1, 1)$ on the unit circle $\{(\cos\theta, \sin\theta, 1) |\ 0 \leq \theta \leq 2\pi\}$. Segment 3 is simply a half-line $\{(0, t, t) |\ t < 0\}$; it is topologically connected to segment 2 at $(0, 0, 0)$, the apex of the cone.

All the algorithms and examples presented in this paper were implemented and created using tools available in the IRIT [4] solid modeling system, developed at the Technion, Israel. The experiments were carried out on a 195 Mhz R10000 SGI machine.

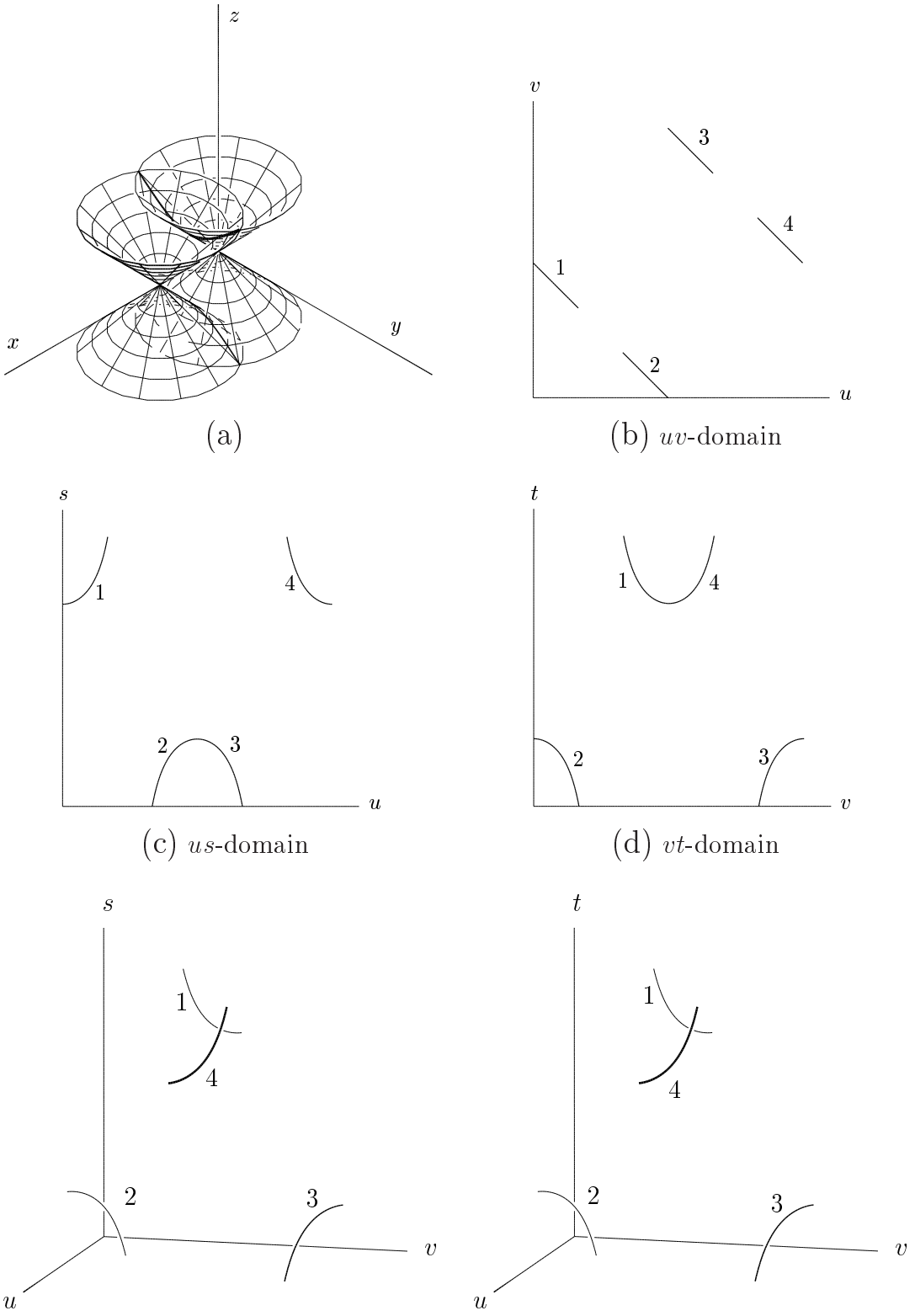

Figure 11: Projections to Different Domains (for Example 1).

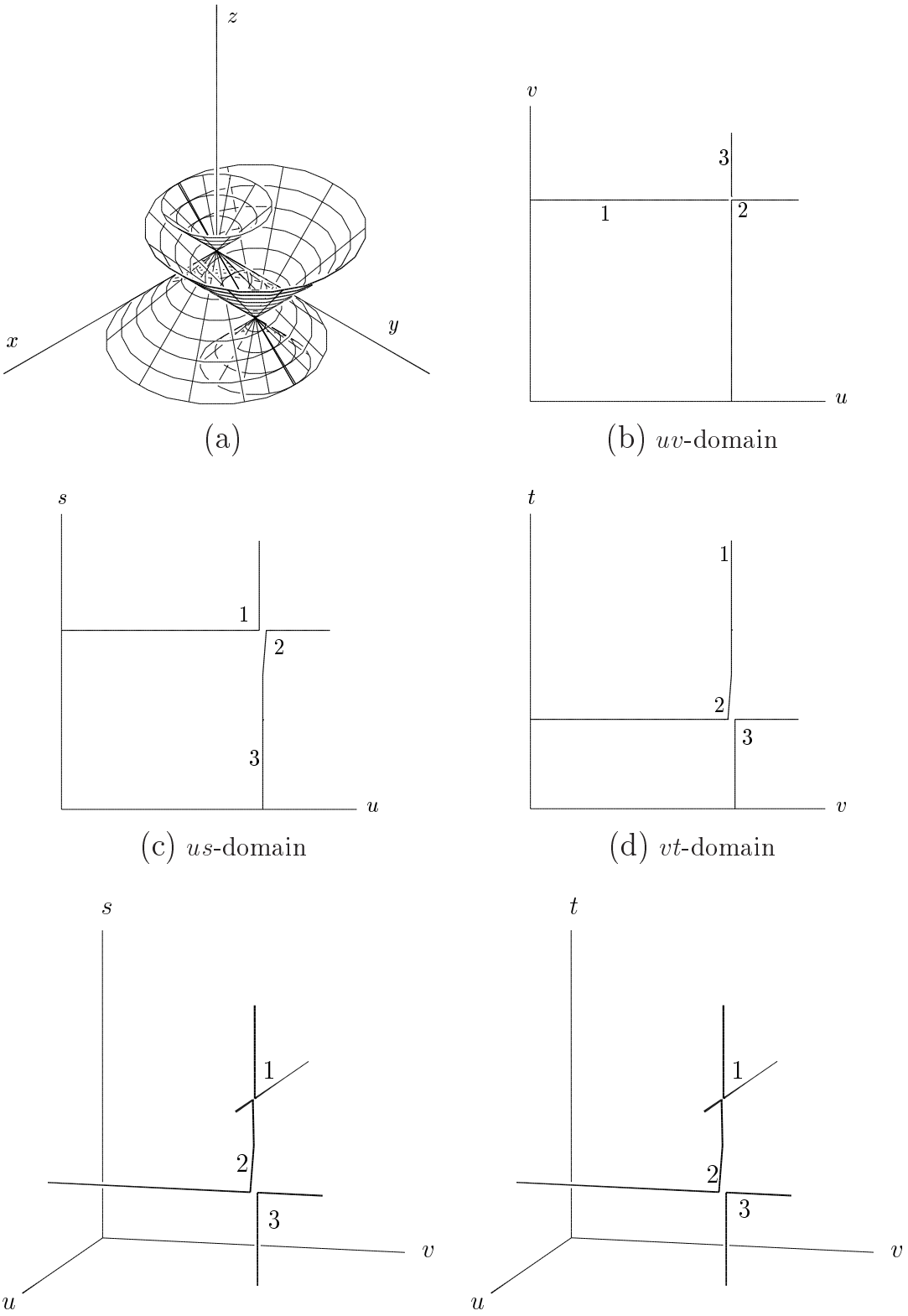

Figure 12: Projections to Different Domains (for Example 2).

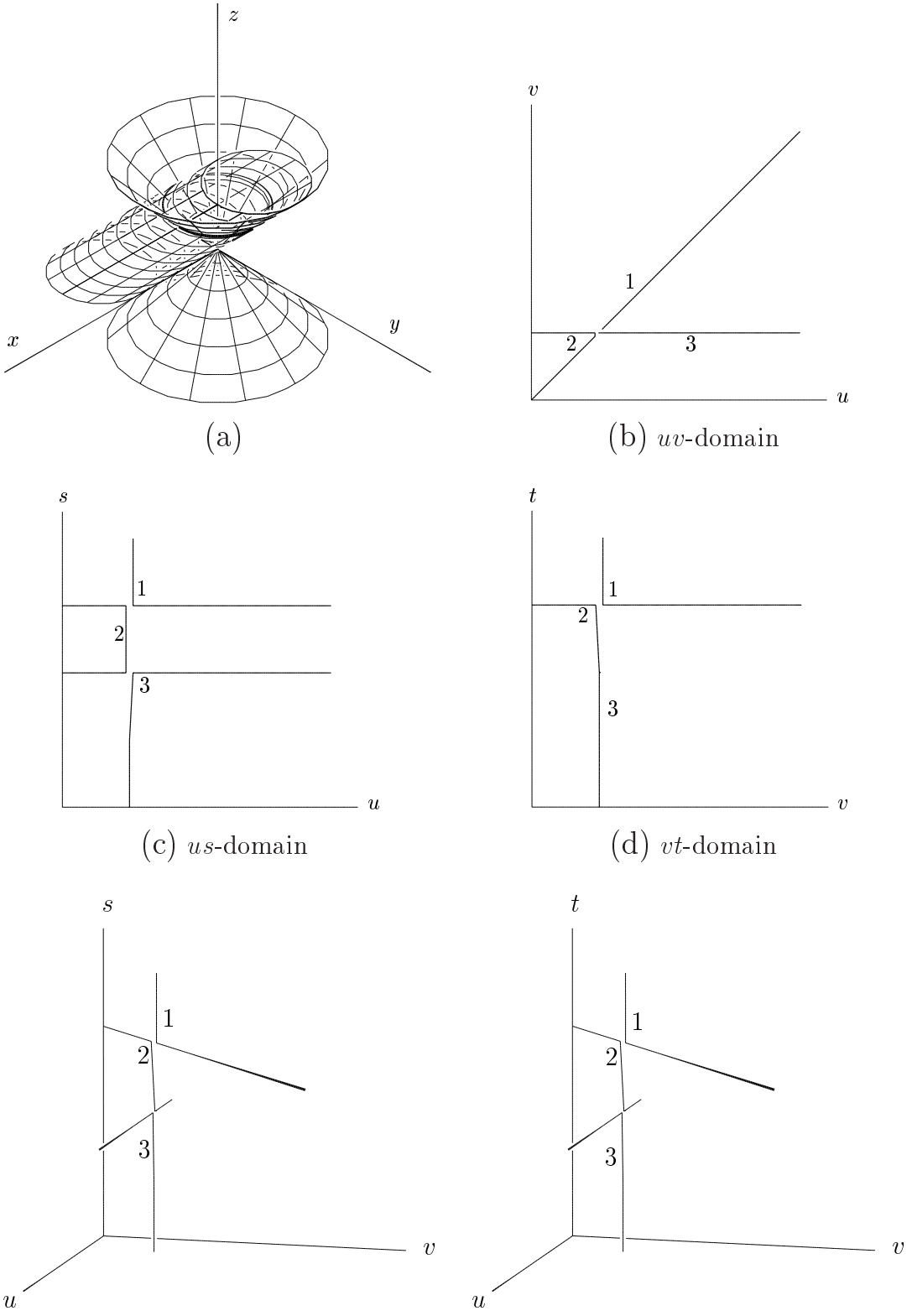

Figure 13: Projections to Different Domains (for Example 3).

5 Conclusion

In this paper, we presented an efficient and robust intersection algorithm for two ruled surfaces. The ruled/ruled surface intersection problem was reformulated as a zero-set finding problem for a bivariate function. The overall computation procedure is numerically stable based on the B-spline subdivision technique.

6 Acknowledgements

The authors would like to thank the anonymous referees for their invaluable comments which were very useful in improving the presentation of this paper from its preliminary version [6].

References

[1] J.-J. Choi, *Local Canonical Cubic Curve Tracing along Surface/Surface Intersections*, Ph.D. Thesis, Dept. of Computer Science, POSTECH, February, 1997.

[2] M. do Carmo, *Differential Geometry of Curves and Surfaces*, Prentice-Hall, Englewood Cliffs, NJ, 1976.

[3] G. Elber and E. Cohen, Second Order Surface Analysis using Hybrid Symbolic and Numeric Operators, *ACM Transactions on Graphics*, **12**(2), 160–178, 1993.

[4] G. Elber, *IRIT 7.0 User's Manual*, Technion, 1996. http://www.cs.technion.ac.il/~irit.

[5] G. Elber and M.-S. Kim, Geometric Shape Recognition of Freeform Curves and Surfaces, *Graphical Models and Image Processing*, **59**(6), 417–433, 1997.

[6] H.-S. Heo, M.-S. Kim, and G. Elber, Ruled/Ruled Surface Intersection, *Proc. of Geometric Modeling and Processing '98*, April 7–8, 1998, Pohang, Korea, pp. 215–223.

[7] J. Hoschek and D. Lasser, *Fundamentals of Computer Aided Geometric Design*, A.K. Peters, Wellesley, MA, 1993.

[8] K.-J. Kim, M.-S. Kim, and K. Oh, Torus/Sphere Intersection Based on a Configuration Space Approach, *Graphical Models and Image Processing*, **60**(1), 77–92, 1998.

[9] K.-J. Kim and M.-S. Kim, Computing All Conic Sections in Torus and Natural Quadric Intersections, *Proc. of Israel-Korea Bi-National Conference on New Themes in Computerized Geometric Modeling*, February 18–19, 1998, Tel-Aviv University, Ramat Aviv, Israel, pp. 11–20.

[10] J. Miller and R. Goldman, Geometric Algorithms for Detecting and Calculating All Conic Sections in the Intersection of Any Two Natural Quadric Surfaces, *Graphical Models and Image Processing*, **57**(1), 55–66, 1995.

[11] H. Pottmann and G. Farin, Developable Rational Bézier and B-spline Surfaces, *Computer Aided Geometric Design*, **12**(5), 513–531, 1995.

[12] H. Pottmann, W. Lü, and B. Ravani, Rational Ruled Surfaces and Their Offsets, *Graphical Models and Image Processing*, **58**(6), 544–552, 1996.

[13] T. Sederberg, H. Christiansen, and S. Katz, Improved Test for Closed Loops in Surface Intersections, *Computer-Aided Design*, **21**(8), 505–508, 1989.

[14] T. Sederberg and T. Satto, Rational-Ruled Surfaces: Implicitization and Section Curves, *Graphical Models and Image Processing*, **57**(4), 334–342, 1995.

[15] C.-K. Shene and J. Johnstone, On the Lower Degree Intersections of Two Natural Quadrics, *ACM Transactions on Graphics*, **13**(4), 400–424, 1994.

A Rational Bilinear Surface

Assume that any two ruling lines $L_1^{u_0}(s)$ and $L_1^{u_1}(s)$ of the ruled surface $S_1(u,s)$ are skew, and any two ruling lines $L_2^{v_0}(t)$ and $L_2^{v_1}(t)$ of the other ruled surface $S_2(v,t)$ are also skew. Moreover, assume that, for each pair (u,v), the two ruling lines $L_1^u(s)$ and $L_2^v(t)$ intersect at a point P_{uv}. Let $S(u,v) = P_{uv}$, for all $(u,v) \in [u_a,u_b] \times [v_a,v_b]$. Below we show that this surface $S(u,v)$ can be represented as a rational bilinear surface. Figure 14 shows the surface $S(u,v)$ bounded by four lines: $L_1^{u_a}(s)$, $L_2^{v_b}(t)$, $L_1^{u_b}(s)$, $L_2^{v_a}(t)$, and four corners: $P_{u_a v_a}$, $P_{u_a v_b}$, $P_{u_b v_b}$, $P_{u_b v_a}$. We consider how to assign weights to these four corner points so that the resulting rational bilinear surface represents the surface $S(u,v)$ exactly.

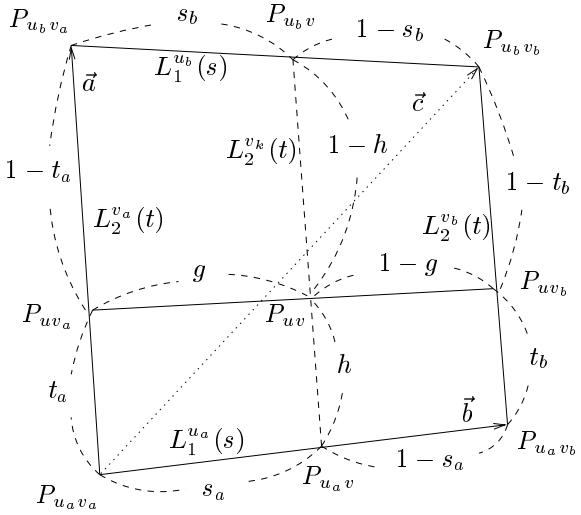

Figure 14: Rational Bilinear Surface

Consider the following three vectors:

$$\begin{aligned}\vec{a} &= \overrightarrow{P_{u_a v_a} P_{u_b v_a}},\\ \vec{b} &= \overrightarrow{P_{u_a v_a} P_{u_a v_b}},\\ \vec{c} &= \overrightarrow{P_{u_a v_a} P_{u_b v_b}}.\end{aligned}$$

Note that these vectors are linearly independent since the lines $L_1^{u_a}(s)$ and $L_1^{u_b}(s)$ are skew. From the configuration given in Figure 14, we can derive the following relations:

$$\begin{aligned}P_{uv_a} - P_{u_a v_a} &= t_a \vec{a},\\ P_{uv_b} - P_{u_a v_a} &= (1-t_b)\vec{b} + t_b \vec{c},\\ P_{u_a v} - P_{u_a v_a} &= s_a \vec{b},\\ P_{u_b v} - P_{u_a v_a} &= (1-s_b)\vec{a} + s_b \vec{c}.\end{aligned}$$

The vector $P_{uv} - P_{u_a v_a}$ can be represented in two different ways:

$$\begin{aligned}P_{uv} - P_{u_a v_a} &= (1-g)(P_{uv_a} - P_{u_a v_a}) + g(P_{uv_b} - P_{u_a v_a})\\ &= (1-g)t_a\vec{a} + g\left[(1-t_b)\vec{b} + t_b\vec{c}\right]\\ &= (1-g)t_a\vec{a} + g(1-t_b)\vec{b} + g t_b \vec{c}\\ P_{uv} - P_{u_a v_a} &= (1-h)(P_{u_a v} - P_{u_a v_a}) + h(P_{u_b v} - P_{u_a v_a})\\ &= (1-h)s_a\vec{b} + h\left[(1-s_b)\vec{a} + s_b\vec{c}\right]\\ &= h(1-s_b)\vec{a} + (1-h)s_a\vec{b} + h s_b \vec{c}\end{aligned}$$

Since the vectors $\vec{a}$, $\vec{b}$, $\vec{c}$ are linearly independent, we have

$$\begin{aligned}(1-g)t_a &= h(1-s_b)\\ g(1-t_b) &= (1-h)s_a\\ gt_b &= hs_b\end{aligned}$$

By eliminating g and h, we get

$$(s_at_a + s_a(s_b-1))t_b = (s_at_a + t_a(t_b-1))s_b,$$

which can be reformulated as follows

$$t_b = \frac{\frac{(1-s_a)/s_a}{(1-s_b)/s_b}t_a}{(1-t_a)+\frac{(1-s_a)/s_a}{(1-s_b)/s_b}t_a} = \frac{wt_a}{(1-t_a)+wt_a},$$

where $w = \frac{(1-s_a)/s_a}{(1-s_b)/s_b}$. It is easy to derive the following equalities:

$$w = \frac{(1-s_a)/s_a}{(1-s_b)/s_b} = \frac{(1-t_a)/t_a}{(1-t_b)/t_b}, \quad s_b = \frac{ws_a}{(1-s_a)+ws_a}.$$

Let's define a rational bilinear surface

$$B(s,t) = \frac{(1-s)(1-t)P_{u_av_a} + s(1-t)P_{u_av_b} + (1-s)tP_{u_bv_a} + stwP_{u_bv_b}}{(1-s)(1-t)+s(1-t)+(1-s)t+stw}.$$

Straightforward computations show that

$$B(0,0) = P_{u_av_a},\ B(1,0) = P_{u_av_b},\ B(0,1) = P_{u_bv_a},\ B(1,1) = P_{u_bv_b}.$$

Thus the bilinear surface $B(s,t)$ interpolate four corners of $S(u,v)$. Moreover, $B(s,t)$ interpolates four boundary lines of $S(u,v)$:

$$\begin{aligned}B(s,0) &= (1-s)P_{u_av_a} + sP_{u_av_b} = P_{u_av_a} + s(P_{u_av_b} - P_{u_av_a})\\ B(0,t) &= (1-t)P_{u_av_a} + tP_{u_bv_a} = P_{u_av_a} + t(P_{u_bv_a} - P_{u_av_a})\\ B(s,1) &= \frac{(1-s)P_{u_bv_a} + swP_{u_bv_b}}{(1-s)+sw} = P_{u_bv_a} + \frac{sw}{(1-s)+sw}(P_{u_bv_b} - P_{u_bv_a})\\ B(1,t) &= \frac{(1-t)P_{u_av_b} + twP_{u_bv_b}}{(1-t)+tw} = P_{u_av_b} + \frac{tw}{(1-t)+tw}(P_{u_bv_b} - P_{u_av_b}).\end{aligned}$$

Note that $B(s,t)$ interpolates the boundary of $S(u,v)$ in the same ratios as shown in Figure 14:

$$B(s_a,0) = P_{u_av},\ B(0,t_a) = P_{uv_a},\ B(s_a,1) = P_{u_bv},\ B(1,t_a) = P_{uv_b}.$$

Thus $B(s,t)$ and $S(u,v)$ generate the same ruled surface. The surface $S(u,v)$ must be a rational bilinear surface.

B Implicitization as a Quadric Surface

Given a rational bilinear surface

$$B(s,t) = \frac{(1-s)(1-t)P_{u_a v_a} + s(1-t)P_{u_a v_b} + (1-s)tP_{u_b v_a} + stwP_{u_b v_b}}{(1-s)(1-t) + s(1-t) + (1-s)t + stw},$$

let (W, X, Y, Z) be a point (in homogeneous coordinate) on the surface $B(s,t)$. Then we have the following relation:

$$\begin{bmatrix} W \\ X \\ Y \\ Z \end{bmatrix} = \begin{bmatrix} 1 & 1 & 1 & w \\ P_{u_a v_a} & P_{u_a v_b} & P_{u_b v_a} & wP_{u_b v_b} \end{bmatrix} \begin{bmatrix} (1-s)(1-t) \\ s(1-t) \\ (1-s)t \\ st \end{bmatrix}, \tag{8}$$

where each point P must be interpreted as a 3×1 submatrix. Note that

$$\begin{aligned} & \det \begin{bmatrix} 1 & 1 & 1 & w \\ P_{u_a v_a} & P_{u_a v_b} & P_{u_b v_a} & wP_{u_b v_b} \end{bmatrix} \\ = & \det \begin{bmatrix} 1 & 0 & 0 & 0 \\ P_{u_a v_a} & P_{u_a v_b} - P_{u_a v_a} & P_{u_b v_a} - P_{u_a v_a} & w(P_{u_b v_b} - P_{u_a v_a}) \end{bmatrix} \\ = & \det \begin{bmatrix} 1 & 0 & 0 & 0 \\ P_{u_a v_a} & \vec{b} & \vec{a} & w\vec{c} \end{bmatrix} \neq 0. \end{aligned}$$

Thus the 4×4 matrix of Equation (8) is invertible. We have the following relation for some 4×4 matrix $A = (a_{ij})$:

$$\begin{bmatrix} (1-s)(1-t) \\ s(1-t) \\ (1-s)t \\ st \end{bmatrix} = A \begin{bmatrix} W \\ X \\ Y \\ Z \end{bmatrix}.$$

When we multiply the first and fourth rows, we get $(1-s)(1-t)st$, which is the same as the multiplication of the second and third rows: $s(1-t)(1-s)t$. As a result, we have

$$\begin{aligned} & (a_{11}W + a_{12}X + a_{13}Y + a_{14}Z)(a_{41}W + a_{42}X + a_{43}Y + a_{44}Z) \\ = & (a_{21}W + a_{22}X + a_{23}Y + a_{24}Z)(a_{31}W + a_{32}X + a_{33}Y + a_{34}Z), \end{aligned}$$

which produces a quadric representation of the rational bilinear surface $B(s,t)$.